Translational Oncology
www.transonc.com

Volume 10 Number 4 August 2017 pp. 518–526 518

Preparation and Identification of HER2 Radioactive Ligands and Imaging Study of Breast Cancer-Bearing Nude Mice[1]

Meng-zhi Zhang*, Yan-xing Guan*, Jin-xiu Zhong† and Xue-zhong Chen*

*Department of Nuclear Medicine, The First Affiliated Hospital of Nanchang University, Nanchang, 330006, China; †Department of Nuclear Medicine, Tumor Hospital of Jiangxi Province, Nanchang, China

Abstract

OBJECTIVE: A micro-molecule peptide TP1623 of ^{99m}Tc-human epithelial growth factor receptor 2 (HER2) was prepared and the feasibility of using it as a HER2-positive molecular imaging agent for breast cancer was evaluated. *METHODS:* TP1623 was chemically synthesized and labeled with ^{99m}Tc. The labeling ratio and stability were detected. HER2 expression levels of breast cancer cells (SKBR3 and MDA-MB-231) and cell binding activity were measured. Biodistribution of ^{99m}TC-TP1623 in normal mice was detected. SKBR3/MDA-MB-231-bearing nude mice models with high/low expressions of HER2 were established. Tumor tissues were stained with hematoxylin–eosin (HE) and measured by immunohistochemistry to confirm the formation of tumors and HER2 expression. SPECT imaging was conducted for HER2-overexpressing SKBR3-bearing nude mice. The T/NT ratio was calculated and compared with that of MDA-MB-231-bearing nude mice with low HER2 expression. The competitive inhibition image was used to discuss the specific binding of ^{99m}Tc- TP1623 and the tumor. *RESULTS:* The labeling ratio of ^{99m}Tc-TP1623, specific activity, and radiochemical purity (RCP) after 6 h at room temperature were (97.39 ± 0.23)%, (24.61 ± 0.06) TBq/mmol, and (93.25 ± 0.06)%, respectively. HER2 of SKBR3 and MDA-MB-231 cells showed high and low expression levels by immunohistochemistry, respectively. The in vitro receptor assays indicated that specific binding of TP1623 and HER2 was retained. Radioactivity in the brain was always at the lowest level, while the clearance rate of blood and the excretion rate of the kidneys were fast. HE staining showed that tumor cells were observed in SKBR3- and MDA-MB-231-bearing nude mice, with significant heteromorphism and increased mitotic count. The imaging of mice showed that targeted images could be made of ^{99m}Tc-TP1623 in high HER2-expressing tumors, while no obvious development was shown in tumors in low HER2-expressing nude mice. No development was visible in tumors in competitive inhibition of imaging, which indicates the combination of ^{99m}Tc-TP1623 and tumor was mediated by HER2. *CONCLUSION:* High labeling ratio and specific activity of ^{99m}Tc-TP1623 is successfully prepared; it is a molecular imaging agent for HER2-positive tumors that has potential applicative value.

Translational Oncology (2017) 10, 518–526

Introduction

Human epithelial growth factor receptor 2 (HER2) has a close relationship with various tumors [1]. HER2 overexpression is found in malignant tumors, such as breast, ovarian, gastric, and colorectal cancers. These tumors have the following features: a high degree of malignancy, strong invasion, easy metastasis, and poor prognosis [2]. Therefore, it is of great significance for the diagnosis of tumors and targeted therapy of HER2 if HER2 is accurately detected. Currently, the most common methods of clinical detection of HER2 are immunohistochemistry and fluorescence in situ hybridization

Address all correspondence to: Yan-xing Guan, PhD, Department of Nuclear Medicine, The First Affiliated Hospital of Nanchang University, NO.17 Yong Wai Street, Nanchang 330006, China.
E-mail: yanxingguan2000@aliyun.com

[1] Funding: This project was supported by 555 Project of Gan Po Elite in Jiangxi Province.
Received 12 January 2017; Revised 10 April 2017; Accepted 12 April 2017

1936-5233/17
http://dx.doi.org/10.1016/j.tranon.2017.04.003

(FISH); both methods have a 20% misdiagnosis rate [3] and lack both comprehensiveness and timeliness [4]. This is because the expression of HER2 in the tumor is heterogeneous, which suggests that the expression of HER2 may be different in primary lesions within the tissue, between the primary tumor and metastases, and between different metastases. However, radionuclide imaging can monitor the expression of HER2 in a living, whole, non-invasive, timely, and effective manner; furthermore, it has the unique advantages of high sensitivity and specificity. Researchers reported the HER2-targeted peptide was used in detecting HER2 expression in mice bearing human breast cancers [5]. At the same time, ^{99m}Tc imaging probes were also applied for measuring HER2 expression in cancer cells [6].

Currently, the main molecular targeting probes for HER2 imaging are monoclonal antibody [7] and micro-molecule peptide. The monoclonal antibody has a large molecular weight (150 kDa) and less quantity penetration into the tumor, with slow blood clearance, long imaging time, low binding affinity to HER2, and low sensitivity. The micro-molecule peptide is obtained from a specific peptide synthesizer. It is easily prepared and stored, and has stable physical properties. Moreover, it has more advantages in clinical application because of its small molecular weight, fast blood clearance, easier binding with the receptor, and high imaging sensitivity.

Alan Berezov et al. [8] found that YCFPDEEGACY, as a small molecular mimic peptide of HER2, had a high affinity for HER2, and could be specifically combined with HER2 to prevent the formation of dimers and inhibit the proliferation of tumor cells. In this study, we prepared and synthesized G (D) AGG-Aba-YCFPDEEGACY-NH2 (TP1623) by chemical modification, and used the G (D) AGG peptide as a bifunctional chelator to achieve the indirect labeling of ^{99m}Tc. We discussed the feasibility of using ^{99m}Tc as a molecular imaging agent for HER2-positive breast cancer.

Materials and Methods

Preparation of ^{99m}Tc-TP1623

YCFPDEEGACY was synthesized by conventional solid-phase synthesis, using a 12-channel semi-automatic peptide synthesizer. The carboxyl terminal of YCFPDEEGACY was amidated. The bifunctional chelator G (D) AGG-Aba- was coupled with an amino terminal. Then, the modified product G (D) AGG-Aba-YCFPDEEGACY-NH2 (since the relative molecular mass was about 1623, it was named TP1623) was obtained. The product was purified by HPLC, and the chemical purity was identified by mass spectrometry.

^{99m}Tc-TP1623 was prepared by an indirect labeling method. The experiment conditions were as follows: 15 μl (15 μg) TP1623 dissolved in an acetic acid buffer (50 mmol/L, PH 4.6), 10 μl (15 μg) tin chloride solution, 300 μl 67 mmol/L sodium phosphate solution, 100 μl $^{99m}TcO_4^-$ (222 MBq, produced by a ^{99}Mo-^{99m}Tc generator of the fission type, Beijing Atom Hi-Tech Company, RCP of $^{99m}TcO_4^-$ > 98%) were sequentially added to a 2.5 ml freezing tube at room temperature. The total volume of reaction was 425 μl, and the PH was 10. The solution was fully mixed, sealed with nitrogen and sealing adhesion, and shaken at room temperature (200 times/min). A label was carried out for 30 min. NaH_2PO_4 (35 μl, 1 mol/L) was added to the labeled ^{99m}Tc-TP1623 solution to adjust the PH (7.0–7.2).

Measuring the Labeling Ratio and Specific Activity of ^{99m}Tc-TP1623

The ^{99m}Tc-TP1623 solution (0.5 μl) was spotted on the origin point of 3 MM chromatographic paper. The mobile phase consisted of acetone (developing solvent I) and developing solvent II (V (30% ammonia):V (absolute ethanol):V (double distilled water) = 1:2:5). A radiation scanner (Bioscan, USA) was used to measure the radioactive count, to obtain the labeling ratio. In developing solvent I, ^{99m}Tc-TP1623 and colloid ^{99m}Tc ($^{99m}TcO2 \bullet xH_2O$, after hydrolysis) were on the origin spot. The R_f value of dissociate ^{99m}Tc was from 0.9–1.0. In developing solvent II, colloid ^{99m}Tc was still on the origin spot. R_f values of ^{99m}Tc-TP1623 and dissociate ^{99m}Tc were from 0.7–0.8 and 0.8–0.9, respectively. The labeling ratio and specific activity were calculated according to the following formulas:

Labeling ratio = 100% – origin radioactive count in developing solvent I (%) – origin radioactive count in developing solvent II (%).

$$\text{specific activity (TBq/mmol)} = \frac{\text{radioactivity}^{99m}\text{Tc(TBq)} \times \text{labeling ratio}}{\text{TP1623chemical quantity(mg)} \times \text{chemical purity/relative molecular mass ofTP1623}}$$

Maximum Activity of the Binding Experiments of ^{99m}Tc

Fresh $^{99m}TcO_4^-$ (222 MBq/100 μl, 370 MBq/100 μl, 740 MBq/100 μl, and 1110 MBq/100 μl) was added to the ^{99m}Tc-TP1623 solution. The labeling rate was observed, and the maximum activity of TP1623 combined with ^{99m}Tc was identified when the labeling rate was >90%.

Measuring the RCP

The chromatographic conditions were as follows: HPLC, Waters 66E Controller pump, HYPERSIL C18 column (250 mm × 4.6 mm, particle size of 5.0 μm), column temperature of 25°C, ultraviolet wavelength λ = 280 nm, the mobile phase A solution was 0.1% trifluoroacetic acid (TFA), the B solution was acetonitrile containing 0.1% TFA, and the elution gradient of B was 10% to 90%. The ^{99m}Tc-TP1623 solution (50 μl) was diluted to 100 μl with a phosphate buffer saline (PBS) solution. A sample of diluent (50 μl) was prepared and added to the pump at room temperature. The flow speed was 0.6 ml/min and the analysis time was 16 min. The eluate was collected with tubes at different periods; each tube had 0.3 ml eluate. The radioactive count (CPM) in each tube was measured by a γ immunoassay instrument (Anhui

ZhongJia Optoelectronic Instrument Company, Hefei, China), and the elution time–radioactivity curve (T–A curve) was drawn. The RCP was calculated according to the following formula:

$$\text{Radiochemical purity (\%)} = \frac{\text{Total CPM of peak labeled products}}{\text{Total CPM of all collection tubes}} \times 100\%$$

Stability Test In Vitro and Serum

The labeled ^{99m}Tc-TP1623 solution was sealed and placed for 0 h, 2 h, 4 h, and 6 h at room temperature before chromatography on 3 MM chromatographic paper. The RCP of ^{99m}Tc-TP1623 at different points in time was measured.

^{99m}Tc-TP1623 solution was mixed with serum from healthy controls at a volume of 1:10. Then, the mixture was filled and sealed with nitrogen and incubated at 37°C. Samples were collected at 1 h, 2 h, 4 h, 6 h and 24 h. RCP of ^{99m}Tc-TP1623 was measured by HPLC.

Identification of Binding Activity of ^{99m}Tc-TP1623 In Vitro Cells

Cell Culture. Human breast cancer SKBR3 cells (Shanghai Cell Bank, Chinese Academy of Sciences, Shanghai) with a high expression of HER2 and MDA-MB-231 cells (Shanghai Cell Bank, Chinese Academy of Sciences, Shanghai) with a low expression of HER2 were cultured using an adherent method. DMEM medium and L-15 medium (containing 10% fetal bovine serum, Gibco) were used and incubated at 37°C with 5% CO_2. When the degree of cell fusion reached about 80%–90%, the mediums were discarded and the cells were washed twice with PBS. Trypsin (0.25%) was added to the cells. When the cells gradually shrank and became rounded with dilated intercellular space, a complete culture medium was added to terminate digestion. Cell suspension was transferred to a sterile centrifuge tube and centrifuged at 1000 rpm for 5 min. After discarding the supernatant, fresh culture medium was added, and cell suspension was passaged at a ratio of 1:2 or 1:3. The shape of the cell and cell viability were observed the next day.

Measuring HER2 Expression in Breast Cancer Cells. The expressions of HER2 in SKBR3 and MDA-MB-231 cells were identified by immunohistochemistry and the flow cytometry method.

Immunohistochemistry. SKBR3 cells and MDA-MB-231 cells in the logarithmic growth phase ($5–10 \times 10^4$) were seeded in a 12-well cell culture plate and incubated at 37°C with 5% CO_2 for 24 h, and then rinsed using PBS and fixed with 4% paraformaldehyde. H_2O_2 (3%), 10% goat serum for blocking, a primary antibody (200 μl, Rabbit anti-c-erbB-2 antibody, Maixin Reagent), and a secondary antibody (200 μl, Goat anti-rabbit, Maixin Reagent) were applied. The cells were incubated, and then rinsed with PBS after each step. Images were observed and collected under a microscope. The semi-quantitative analysis was analyzed by two experienced pathologists, according to the proportion of positive cells and the intensity of staining. The scoring guidelines of the proportion of positive cells are: 0, a proportion <10%; 1, a proportion of 10%–40%; 2, a proportion of 40%–70%; 3, a proportion ≥70%. The scoring guidelines of the intensity of staining are: 0, no staining; 1, light yellow; 2, brown-yellow; 3, brown. The two kinds of scores were added. A score of 0–1 was interpreted as negative (–); a score of 2, low expression (+); scores of 3–4, positive expression (++); scores of 5–6, strong positive expression (+++).

Binding Assay of ^{99m}Tc-TP1623 and HER2 In Vitro. SKBR3 cells were seeded in 24-well plates one day before the experiment. ^{99m}Tc-TP1623 was added to each well on the second day. The final concentrations were 0.5, 1, 5, 10, 50, 100, 200, and 400 nmol/L, with three repetitions in each concentration. In the non-specific binding group, 300–500 times of the TP1623 was added to each well. One hour later, the same amount of ^{99m}Tc-TP1623 was added to each well and incubated for 2 h at 4°C. It was then rinsed three times, using ice-cold PBS (containing 0.1% Bull Serum Albumin). The CPM was measured by a γ immuno counter. The total binding count (TB) minus the non-specific binding group count (NSB) was the specific binding (SB) of the radioactive count. Graphpad pism 5.0 (GraphPad, San Diego, CA) was used for simulating the saturation curve.

SKBR3 cells ($2–4 \times 10^4$ cells/well) were seeded in 24-well plates on the first day. TP1623 was added to each well on the second day. The final concentrations were 0, 1, 5, 25, 50, 500 nmol/L, with three repetitions in each concentration, placed at 4°C for 30 minutes. ^{99m}Tc-TP1623 (462 KBq/0.1 μg/50 μl) was added, incubated for 2 h at 4°C, and rinsed three times using ice-cold PBS. The CPM was measured by a γ immuno counter after digestion with trypsin. The competitive binding curve was drawn (using the TP1623 concentration as the abscissa and the radioactive count as the vertical axis).

Internalization Experiment of ^{99m}TC-TP1623

SKBR3 cells at logarithmic phase were digested and seeded at 6-well plates at a concentration of 5×10^5/L. When the cells reached 80% confluence, the supernatant was discarded. Diluted ^{99m}Tc-TP1623 solution (222KBq/15 ng, 50 μl) was added into each well and cultivated in 5% CO_2 incubator under 37°C. The culture plates were collected at 1 h, 4 h, 8 h, 24 h, the medium was discarded, and the plates were washed with serum-free medium. Glycine (0.2 mol/L, containing 4 mol/L, PH2.5) was added, and the acidic solution was collected after 5 min. The glycine (0.5 mL) was added again, and radioactive counts measured by glycine represented the labeled ^{99m}Tc-TP1623 combined in the cell membrane. Lysis buffer (NaOH, 1 mol/L, 0.5 mL) was added into plates and incubated at 37°C for 30 min. The reacted lysis buffer was collected and washed with 0.5 mL NaOH. The 1 mL NaOH solution represented the cellular internalization of labeled ^{99m}Tc-TP1623.

Internalization percentage of ^{99m}Tc-TP1623 = cellular internalization counts/(cellular internalization counts + cell membrane counts) × 100%.

Measuring Biodistribution of ^{99m}TC-TP1623 in Normal Mice

Thirty KM mice were divided into six groups, with five mice in each group. ^{99m}Tc-TP1623 (3.7 KBq, 100 μl) was injected via the tail vein. Blood, heart, lung, liver, kidney, intestine, muscle, bone, and brain tissue were collected 1, 5, 10, 30, 60, and 120 min after injection. The weight and radioactivity were measured, and converted to the percentage of injection dose per gram (% ID/g).

$$\text{Percentage of injection dose per gram (\%ID/g)} = \frac{\text{Radioactive counts} \times 100}{\text{Weight} \times \text{Reference Source Count}}$$

Observation the Combining Site of ^{99m}Tc-TP1623 and Breast Cancer Cells

SKBR3 and MDA-MB-231 cells were seeded in 12-well plates at a concentration of 1×10^5/L. FITC-TP1623 solution (200 μg) and Hoechst 33,342 (1 mmol/L) were added into each well and cultured at 4°C for 120 min. The medium was discarded, and cells were washed with PBS. The combining site of ^{99m}Tc-TP1623 and SKBR3 and MDA-MB-231 cells were observed under confocal microscope (Wetzler, Heidelberg, Germany).

Establishment of Breast Cancer-Bearing Nude Mice Model

This animal experiment was approved by Ethics Review Committees of Animal Research Institution of The First Affiliated Hospital of Nanchang University. Human breast cancer SKBR3 cells and MDA-MB-231 cells were collected in the logarithmic growth phase, digested with trypsin, centrifuged at 1000 rpm for 5 min, and resuspended in PBS. Cells (5×10^6/150 μl) were inoculated in the axillary of BALB/c nude mice (female, 20–22 g, 6–8 weeks, Beijing Huafukang Biotech). When the tumor diameter >1 cm (usually 4–6 weeks), the mice could be used in this experiment. When the experiment was finished, part of the tumor tissue was cut and made into paraffin sections. The pathology of the tumor and immunohistochemical analysis of HER2 expression was analyzed to confirm the establishment of high and low expressions of HER2 breast cancer-bearing nude mice models.

Imaging Assays

Five SKBR3-bearing nude mice with high expressions of HER2 were injected with 37 MBq/200 μl of ^{99m}Tc-TP1623 through the tail vein, and whole-body dynamic imaging was conducted at 30, 60, 90, 120, 180, and 240 min by SPECT (Symbian T6, Siemens). The SPECT probe was equipped with a pinhole collimator, 140 KeV of energy peak, 20% of window width, 128 × 128 of matrix, and 1.23 of amplification factor. After the calibration of time decay, 1 frame was gathered every 5 min. The T/NT ratio was measured by a region of interest (ROI) technique, and the ratio of T/NT (n) at different times before the block was obtained. Competitive inhibition imaging of these five nude mice was conducted three days later. TP1623 (1500 μg) was injected through the tail vein to block the HER2. One hour later, the same amount of ^{99m}Tc-TP1623 was injected for the dynamic imaging of each phase; the imaging conditions, data acquisition, and image processing remained unchanged. In addition, five MDA-MB-231-bearing nude mice with low expressions of HER2 were used as the negative control group. The conditions and methods were the same as those of the SKBR3-bearing nude mice with high expressions of HER2 before blocking.

Statistical Analysis

We used SPSS 17.0 for the data analysis. Measurement data were expressed as mean ± SD. T/NT at different times before and after blocking was analyzed by one-way ANOVA, and T/NT at the same time of the SKBR3 group and the MDA-MB-231 group was analyzed by t-test, with $P < .05$ considered statistically significant.

Results

Labeling Ratio, Specific Activity and In Vitro and Serum Stability

Different concentrations (222, 370, 740, 1110 MBq/100 μl) of ^{99m}Tc were added to measure the labeling ratio of ^{99m}Tc-TP1623. When the concentration of ^{99m}Tc was 222 MBq/100 μl, the labeling ratio of ^{99m}Tc-TP1623 was the highest (97.39 ± 0.23%) and the specific activity was also the highest (24.61 ± 0.06). When the concentration of ^{99m}Tc was 1110 MBq/100 μl, the labeling ratio of ^{99m}Tc-TP1623 was (93.69 ± 0.98)% and the specific activity was also (24.07 ± 0.44). Hence, the optimal imaging dose of ^{99m}Tc-TP1623 was 222 MBq/15 μg (Table 1). The results of in vitro stability showed that RCPs were (93.66 ± 2.49)%, (93.28 ± 1.08)%, and (93.25 ± 0.06)% after ^{99m}Tc-TP1623 was placed for 2 h, 4 h and 6 h at room temperature (Table 2). RCPs of the mixtures at 1 h, 2 h, 4 h, 6 h and 24 h were (97.14 ± 0.45)%, (93.36 ± 1.78)%, (92.81 ± 0.32)%, (90.57 ± 0.67)% and (86.02 ± 1.34)% (Figure 1),

Table 1. Labeling Rate of ^{99m}Tc-TP1623 at Different Radioactive Concentration (n = 3)

Number	Radioactive Concentration of ^{99m}Tc-TP1623 (MBq/100ul/15 μg)	Labeling Rate (%)
1	222	97.39 ± 0.23
2	370	96.25 ± 0.10
3	740	94.45 ± 0.91
4	1110	93.69 ± 0.98

Table 2. Stability of ^{99m}Tc-TP1623 at Romm Temperature (n = 3)

Time (h)	0	2	4	6
RCP (%)	97.39 ± 0.23	93.66 ± 2.49	93.28 ± 1.08	93.25 ± 0.06

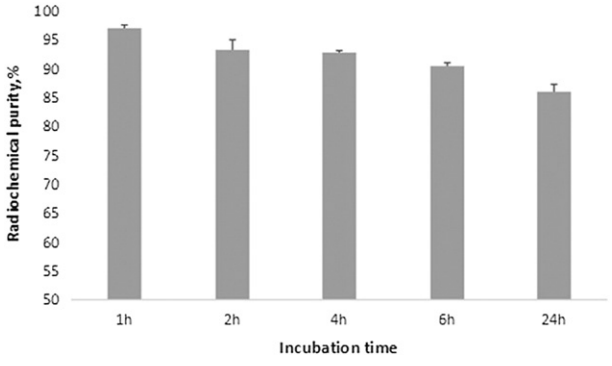

Figure 1. The stability of ^{99m}Tc-TP1623 in serum.

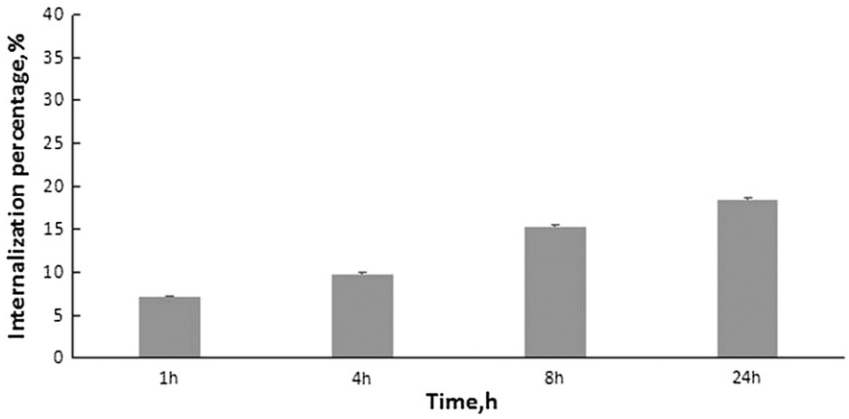

Figure 2. The internalization percentage of ^{99m}Tc-TP1623 in SKBR3 cells.

which indicated that ^{99m}Tc-TP1623 still maintained good stability in serum, and could resist the decomposition of serum protease in serum.

Internalization Percentage of ^{99m}Tc-TP1623 in HER2 Positive Cancer Cells

Internalization percentages of ^{99m}Tc-TP1623 at 1 h, 4 h, 8 h, and 24 h were (7.21 ± 0.09)%, (9.81 ± 0.17)%, (15.35 ± 0.20)% and (18.41 ± 0.27)% (Figure 2), which indicated that the amount of ^{99m}Tc-TP1623 internalized into cells was low, most of ^{99m}Tc-TP1623was closely combined with HER2 on the surface of the cell.

Combining Activity of ^{99m}Tc-TP1623 and HER2

Immunohistochemistry showed strong positive (+++) HER2 expression in SKBR3 cells (Figure 3*A*) and negative or low (−/+) HER2 expression in MDA-MB-231 cells (Figure 3*B*). The in vitro receptor saturation experiment showed, with the increase of ^{99m}Tc-TP1623 concentration, the binding rate of HER2 and ^{99m}Tc-TP1623 was gradually increased until saturation (Figure 3*C*). The in vitro receptor competitive assay showed, with the increase of TP1623 concentration, the binding rate of HER2 and ^{99m}Tc-TP1623 was gradually decreased; it showed concentration dependence (Figure 3*D*), which indicated that TP1623 could competitively inhibit the binding of ^{99m}Tc-TP1623 and HER2 receptors.

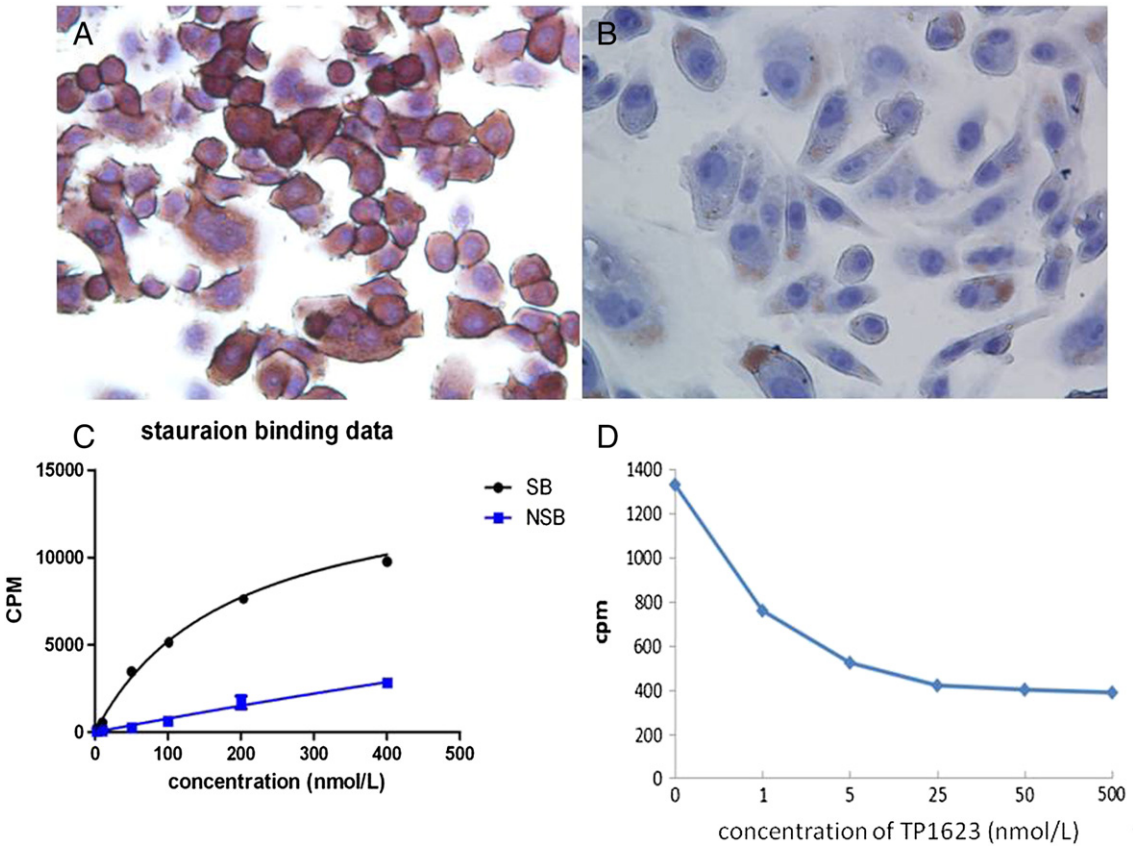

Figure 3. Combining activity of ^{99m}Tc-TP1623 and HER2. A. Immunohistochemical analysis of HER2 receptor of SKBR3 cells (+++) (original magnification ×400). B. Immunohistochemical analysis of HER2 receptor of MDA-MB-231 cells (−) (original magnification ×400). C. Receptor saturation curve in SKBR3 cells in vitro. D. Receptor competitive curve in SKBR3 cells in vitro.

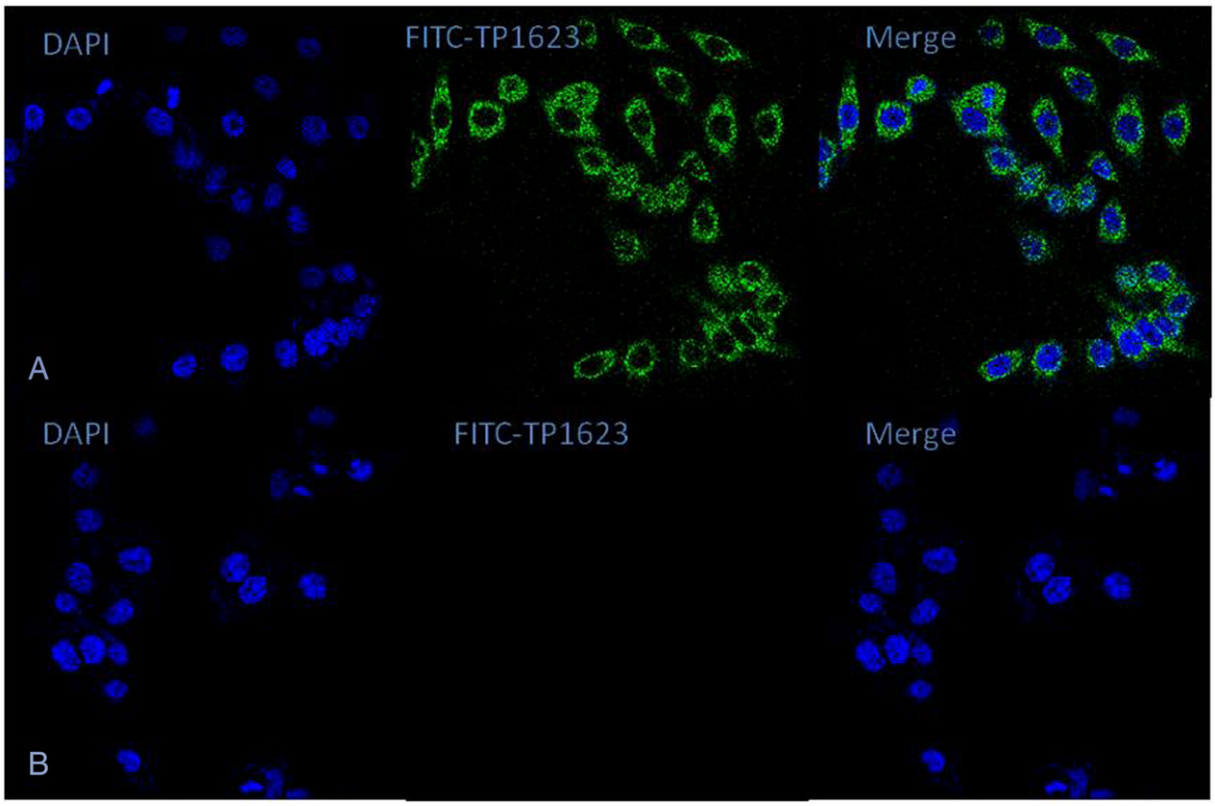

Figure 4. A. Fluorescence microscopy images of HER2-positive cells (SKBR3) incubated with fluorescently labeled TP1623. B. Fluorescence microscopy images of HER2-negative cells (MDA-MB-231) incubated with fluorescently labeled TP1623.

Combining Site of ^{99m}Tc-TP1623 and Breast Cancer Cells

Fluorescence microscopy images of SKBR3 and MDA-MB-231 cells incubated with fluorescently labeled TP1623 were shown in Figure 4. We found fluorescent signal mainly concentrated on the cell membrane, and a small amount of signal concentrated on the cytoplasm. No obvious signal was observed in the membrane and cytoplasm of MDA-MB-231 cell, suggesting that ^{99m}Tc-TP1623 was specifically combined with HER2 on the surface of cell membrane.

Biodistribution of ^{99m}TC-TP1623 in Normal Mice

At the start, ^{99m}TC-TP1623 was mainly distributed in the kidneys, lungs, heart, blood, and liver. Five minutes later, radioactivity of ^{99m}TC-TP1623 in the lungs, heart, blood, and liver was gradually decreased with time. Sixty minutes later, radioactivity in those organs was significantly lower than normal, while radioactivity in the brain remained consistently at the lowest level. The clearance rate of blood was fast. The radioactivity at 60 min was 3.42% of that at 1 min. The excretion rate of the kidneys was also fast. Radioactivity was as high as 29.4% ID/g at 10 min, and decreased 77.0% at 120 min. Radioactivity in the intestine grew slowly, increasing 63.14% at 120 min (Table 3).

Establishment of Breast Cancer-Bearing Nude Mice Model

In the HE staining, SKBR3 cells in nude mice had significant heteromorphy characterization and increased mitotic count (Figure 5*A*). The MDA-MB-231 cells in nude mice had similar characteristics (Figure 5*C*). In immunohistochemistry, chocolate brown was visible in the membrane and cytoplasm of SKBR3 cells in nude mice, and SKBR3 tissues showed strong positive (+++) HER2 expression (Figure 5*B*). Small brown particles were visible in the membrane and cytoplasm of MDA-MB-231 cells in nude mice, and MDA-MB-231 tissues showed low (+) HER2 expression (Figure 5*D*).

SPECT/CT Imaging of Tumor-Bearing Nude Mice

In the non-blocking group, images of SKBR3 human breast cancer nude mice with high expressions of HER2 are shown in Figure 6*A*. The images of tumors were visible at 30 min after injection of ^{99m}TC-TP1623. The distribution of tumor radioactivity increased with time, and reached the peak at 120 min (T/NT was 5.18). Following this, the distribution of nuclide slowly decreased; the nuclide was still visible at 4 h (T/NT was 3.49) (Figure 6*A*, Table 4).

In the blocking group, tumor development, and radioactive distribution was significantly reduced. There were no significant changes

Table 3. Biodistribution of ^{99m}TC-TP1623 in Normal Mice at Different Times (% ID/g, $\bar{x} \pm s$)

Time After Injection (min)	Blood	Heart	Lung	Liver	Intestine	Kidney	Muscle	Bone	Brain
1	11.69 ± 1.91	7.13 ± 0.67	13.98 ± 1.74	6.36 ± 1.27	0.75 ± 0.05	22.90 ± 6.00	4.52 ± 0.79	3.06 ± 0.49	0.48 ± 0.05
5	7.38 ± 1.24	3.16 ± 1.67	8.31 ± 1.75	4.41 ± 4.41	0.54 ± 0.06	27.96 ± 3.40	2.93 ± 0.78	2.22 ± 0.41	0.29 ± 0.08
10	4.73 ± 0.79	1.90 ± 0.28	5.43 ± 1.10	3.56 ± 0.43	0.73 ± 0.11	29.35 ± 4.17	2.47 ± 0.69	1.60 ± 0.55	0.23 ± 0.09
30	1.00 ± 0.03	0.47 ± 0.03	1.23 ± 0.12	1.69 ± 0.52	0.77 ± 0.18	20.98 ± 3.22	1.36 ± 0.27	0.35 ± 0.25	0.04 ± 0.02
60	0.40 ± 0.07	0.23 ± 0.07	0.55 ± 0.08	0.57 ± 0.26	0.70 ± 0.34	12.61 ± 2.13	0.81 ± 0.40	0.15 ± 0.09	0.02 ± 0.01
120	0.16 ± 0.03	0.12 ± 0.03	0.30 ± 0.06	0.54 ± 0.29	1.38 ± 0.04	6.75 ± 2.22	0.53 ± 0.14	0.07 ± 0.02	0.01 ± 0.00

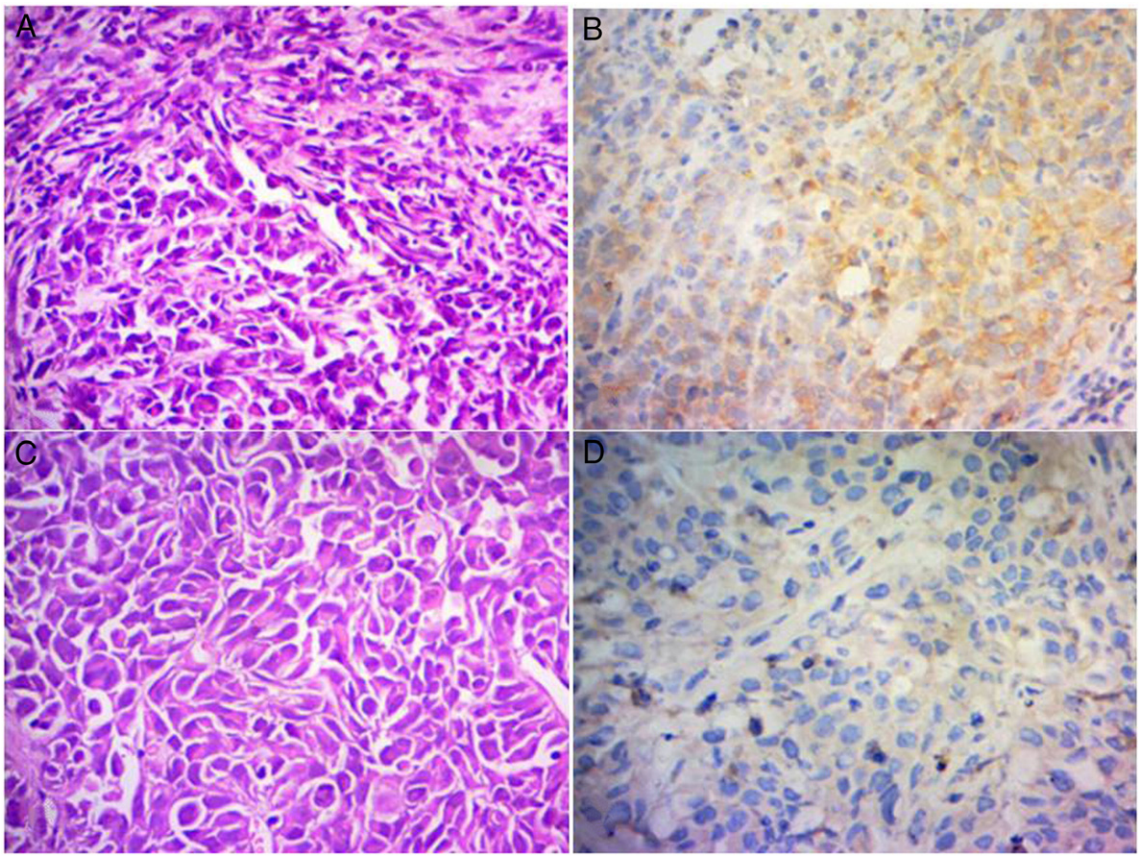

Figure 5. HER2 expressions of SKBR3 and MDA-MB-231 cells. A. HE staining of SKBR3 cells in cancer-bearing nude mice (original magnification ×400). Tumor cells had significant heteromorphy characterization and increased mitotic count. B. Immunohistochemistry of SKBR3 cells in cancer-bearing nude mice. Chocolate brown was visible in membrane and cytoplasm of tumor cells in SKBR3 nude mice, and it showed strong positive (+++) HER2 expression in SKBR3 cells (original magnification ×400). C. HE staining of MDA-MB-231 cells in cancer-bearing nude mice (original magnification ×400). Tumor cells had significant heteromorphy characterization and increased mitotic count. D. Immunohistochemistry of MDA-MB-231 cells in cancer-bearing nude mice. Little brown particles were visible in membrane and cytoplasm of tumor cells in MDA-MB-231 nude mice, and it showed low (+) HER2 expression in MDA-MB-231 cells (original magnification ×400).

in the distribution of radioactivity in the blocking group (T/NT was 1.03 at 120 min and inhibition rate was 80.12%, as shown in Table 4). There was still no significant distribution of nuclide at 4 h (Figure 6*B*). These results indicated that ^{99m}Tc-TP1623 could compete with TP1623 to bind to HER2 in tumor tissue, suggesting that the combination of ^{99m}Tc-TP1623 and tumor was mediated by the HER2 receptor. The specific inhibition rates at different times are shown in Table 4.

Images of MDA-MB-231-bearing nude mice with low expressions of HER2 are shown in Figure 6*C*. There was no radioactive image of the tumor after injection of ^{99m}Tc-TP1623 at different phases. The distribution of radioactivity was sparse in the brain, thyroid, lungs and muscles, and accumulated in the kidneys and bladder. These results indicated that ^{99m}Tc-TP1623 could combine specifically with the HER2 receptor.

Discussion

Breast cancer is one of the most common malignancies in women; its incidence rate ranks second of all female malignant tumors [9]. HER2 is the most important breast cancer-causing gene. Research has found that overexpression of the HER2 gene occurs in 25% to 30% of breast cancer [10]. These tumors are characterized by a high degree of malignancy, rapid progress, and early metastasis and recurrence, with a low survival rate in patients [11]. In recent years, many monoclonal antibodies, their conjugates, small molecule peptides, and peptide vaccines targeting the extracellular binding domain of the HER2 have been developed and applied in clinical studies. Trastuzumab is a humanized monoclonal antibody with high affinity for HER2. Research has found that targeted therapy for HER2-positive patients can significantly improve the survival rate [12,13]. Hence, accurate and timely monitoring of dynamic changes of HER2 in HER2-overexpressing tumors is important for targeted therapy, patient prognosis, efficacy evaluation, and promotion of such therapy.

However, monoclonal antibody therapy has many drawbacks, such as high molecular weight, slow blood clearance rate, high background, long time interval of image acquisition, low image quality, and high dose of radiation [14–16]. YCFPDEEGACY has small molecular weight and a stable structure, so it can pass through the biological barrier quickly. It can combine with HER2 with high affinity and specificity, and further prevent the dimerization of receptors [8,17], thus effectively inhibiting the growth of HER2-positive tumor cells.

Currently, there are two methods for labeling ^{99m}Tc peptides: direct labeling and indirect labeling. In the direct method, ^{99m}Tc is directly linked to the peptide [18] with a low labeling rate and unstable labels, which may destroy the binding sites of the peptide and the HER2 receptor. In the indirect method, ^{99m}Tc and the ligand are connected by a bifunctional chelating agent. This method

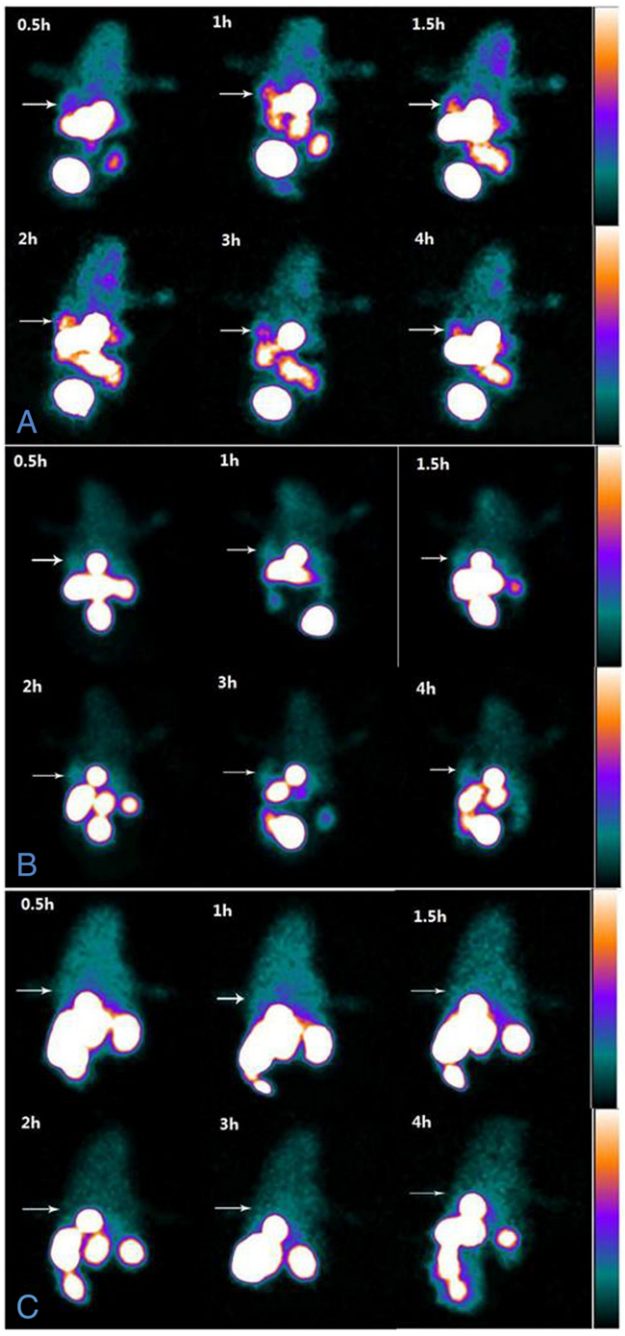

Figure 6. A. SPECT images of SKBR3-bearing nude mice in non-blocking group. The images of tumors were visible at 30 min, reached the peak at 120 min (arrow), and the nuclide was still visible at 4 h. A-C, Scar bars,~500 μm. B. SPECT images of SKBR3-bearing nude mice in blocking group. Radioactive concentration in tumor was significantly reduced at 0.5 h, development of tumor was significantly inhibited at 2 h (arrow). C. SPECT images of MDA-MB-231-bearing nude mice. There was no radioactive concentration in tumor (arrow).

is simple, and the reaction condition is mild with the high-labeled product. Hence, we used the indirect method in this study to avoid the effect of ^{99m}Tc labeling on the biological activity of the peptide and the target molecule. Chelating agent G (D) AGG with an N4 structure was used in this study. The advantages are: a simple chelating agent labeling method of the N4 structure, mild reaction, and easy operation [19]; this can help to avoid many problems in the use of traditional chelating agents (such as maGGG [20], maSSS [20,21]).

Table 4. Inhibition Rates at Different Times Before and After Blocking

Time	T/NT Value Before Blocking (Mean Value)	T/NT Value After Blocking (Mean Value)	Inhibition Rate (%)
30 min	2.19	1.03	52.96
60 min	4.23	1.15	72.81
90 min	4.56	1.06	76.75
120 min	5.18	1.03	80.12
180 min	4.07	1.12	72.48
240 min	3.49	1.08	69.05

Inhibition rate (%) = (T/NT value before blocking- T/NT value after blocking)/T/NT value before blocking.

We synthesized YCFPDEEGACY using a peptide solid-phase chemical method. The labeling ratio of ^{99m}Tc-TP1623 was high to (97.39 ± 0.23)%, which laid the foundation for freeze-dried kits. The specific activity of ^{99m}Tc-TP1623 was (24.61 ± 0.06) TBq/mmol, which could be further used without separation and purification, and can meet the requirements for receptor analysis in vivo and vitro. The labeling ratio was (93.25 ± 0.06)% after being placed for 6 h, which indicates that the labeled peptide had good stability in vitro. Peptides (15 μg) could bind to 1110 MBq (30 mci) ^{99m}Tc provided that the labeling ratio of clinical imaging was more than 90%, which may be used for further clinical research.

In the in vitro receptor saturation and competitive experiment, ^{99m}Tc-TP1623 could bind specifically to SKBR3 cells with a positive expression of HER2, which indicates that ^{99m}Tc-TP1623 maintained the biological activity of the peptide. The specificity, saturation, and competition of ^{99m}Tc-TP1623 and HER2 provided the basis for the application of HER2 imaging in vivo.

The results of HER2 expression, which were determined by HE staining and immunohistochemistry in the nude mice model, were consistent with the results of HER2 expression in vitro. This showed the establishment of the animal model was successful, which provided the basis for the imaging of nude mice.

The ideal targeting probe not only needs to bind to the target with high specificity and high affinity, but must also meet the requirements of good stability, low blood-pool background, and fast excretion through the urinary system. In the entire imaging process, the thyroid and gastric area always showed a soft tissue background, which indicates that the combination of ^{99m}Tc and TP1623 was strong, with no significant shedding of ^{99m}Tc; this suggests that the molecular probe had good stability in vivo. The lungs, neck, limbs, and muscles always showed a soft tissue background, which indicates a fast clearance rate of the molecular probe in the blood. The brain showed a low radioactive background, suggesting that the labels could not cross the blood–brain barrier, and could be used to assess the integrity of the blood–brain barrier. The relative molecular weight of ^{99m}Tc-TP1623 is small, and strong radioisotope concentration was always seen in the kidneys and bladder parts, indicating that the molecular probe was excreted through the urinary system; this helped to get the ideal low blood-pool background image in a short time. Unfortunately, long-term nuclide retention in the kidneys and bladder limited the detection of nearby HER2. Hence, the clearance speed of molecular probes in the kidney and bladder should be further increased.

In summary, the labeling method of ^{99m}Tc-TP1623 is simple with a high labeling ratio (>95%). It can be used without isolation and purification, which indicates it will make an easily prepared one-step freeze-dried kit. The specific activity is high, which can meet the imaging requirements of receptors in vivo and vitro. The

good biological activity of ^{99m}Tc bound to HER2 is retained after labeling TP1623. Moreover, ^{99m}Tc-TP1623 can bind to target tissue rapidly, with clear tumor development and high T/NT ratio, which proves that ^{99m}Tc-TP1623 combined with the tumor is mediated by HER2.

Conclusion

^{99m}Tc-TP1623 is a potential molecular imaging agent for HER2 positive tumors; this lays the foundation for the imaging transformation of such tumors, to provide an objective basis for tumor-targeted diagnosis and early individualized anti-HER2 therapy.

Conflict of Interest

All authors declare that there is no conflict of interest.

Ethical Approval

This animal experiment was approved by Ethics Review Committees of Animal Research Institution of The First Affiliated Hospital of Nanchang University.

Acknowledgement

We wish to thank Prof. Qianwei Li of the Nuclear Medicine Department of Southwest Hospital, Third Military Medical University, for his assistance in providing guidance in experimental design and technology.

References

[1] Ramieri MT, Murari R, Botti C, Pica E, Zotti G, and Alo PL (2010). Detection of HER2 amplification using the SISH technique in breast, colon, prostate, lung and ovarian carcinoma. *Anticancer Res* **30**(4), 1287–1292.

[2] Carlsson J (2012). Potential for clinical radionuclide-based imaging and therapy of common cancers expressing EGFR-family receptors. *Tumor Biol* **33**(3), 653–659.

[3] Yarden Y and Sliwkowski MX (2001). Untangling the ErbB signalling network. *Nat Rev Mol Cell Biol* **2**(2), 127–137.

[4] Aurilio G, Disalvatore D, Pruneri G, Bagnardi V, Viale G, Curigliano G, Adamoli L, Munzone E, Sciandivasci A, and De Vita F, et al (2013). A meta-analysis of oestrogen receptor, progesterone receptor and human epidermal growth factor receptor 2 discordance between primary breast cancer and metastases. *Eur J Cancer* **50**(2), 277–289.

[5] Andersson KG, Oroujeni M, Garousi J, Mitran B, Ståhl S, Orlova A, Löfblom J, and Tolmachev V (2016). Feasibility of imaging of epidermal growth factor receptor expression with ZEGFR:2377 affibody molecule labeled with 99mTc using a peptide-based cysteine-containing chelator. *Int J Oncol* **49**(6), 2285–2293.

[6] Yamaguchi H, Tsuchimochi M, Hayama K, Kawase T, and Tsubokawa N (2016). Dual-Labeled Near-Infrared/99mTc Imaging Probes Using PAMAM-Coated Silica Nanoparticles for the Imaging of HER2-Expressing Cancer Cells. *Int J Mol Sci* **17**(7), 1086.

[7] Boswell CA and Brechbiel MW (2007). Development of radioimmunotherapeutic and diagnostic antibodies: an inside-out view. *Nucl Med Biol* **34**(7), 757–778.

[8] Berezov A, Chen J, Liu Q, Zhang HT, Greene MI, and Murali R (2002). Disabling receptor ensembles with rationally designed interface peptidomimetics. *J Biol Chem* **277**(31), 28330–28339.

[9] Dubey AK, Gupta U, and Jain S (2015). Breast cancer statistics and prediction methodology: a systematic review and analysis. *Asian Pac J Cancer Prev* **16**(10), 4237–4245.

[10] Taskar KS, Rudraraju V, Mittapalli RK, Samala R, Thorsheim HR, Lockman J, Gril B, Hua E, Palmieri D, and Polli JW, et al (2012). Lapatinib Distribution in HER2 Overexpressing Experimental Brain Metastases of Breast Cancer. *Pharm Res* **29**(3), 770–781.

[11] Dean-Colomb W and Esteva FJ (2008). Her2-positive breast cancer: herceptin and beyond. *Eur J Cancer* **44**(18), 2806–2812.

[12] Hudis CA (2007). Trastuzumab—mechanism of action and use in clinical practice. *N Engl J Med* **357**(1), 39–51.

[13] Bang YJ, Van Cutsem E, Feyereislova A, Chung HC, Shen L, Sawaki A, Lordick F, Ohtsu A, Omuro Y, and Satoh T, et al (2010). Trastuzumab in combination with chemotherapy versus chemotherapy alone for treatment of HER2-positive advanced gastric or gastro-oesophageal junction cancer (ToGA): a phase 3, open-label, randomised controlled trial. *Lancet* **376**(9742), 687–697.

[14] Dijkers EC, Oude Munnink TH, Kosterink JG, Brouwers AH, Jager PL, de Jong JR, van Dongen GA, Schröder CP, Lub-de Hooge MN, and de Vries EG, et al (2010). Biodistribution of 89Zr-trastuzumab and PET imaging of HER2-positive lesions in patients with metastatic breast cancer. *Clin Pharmacol Ther* **87**(5), 586–592.

[15] Tamura K, Kurihara H, Yonemori K, Tsuda H, Suzuki J, Kono Y, Honda N, Kodaira M, Yamamoto H, and Yunokawa M, et al (2013). 64Cu-DOTA--trastuzumab PET imaging in patients with HER2-positive breast cancer. *J Nucl Med* **54**(11), 1869–1875.

[16] Mortimer JE, Bading JR, Colcher DM, Conti PS, Frankel PH, Carroll MI, Tong S, Poku E, Miles JK, and Shively JE, et al (2014). Functional imaging of human epidermal growth factor receptor 2-positive metastatic breast cancer using (64)Cu-DOTA-trastuzumab PET. *J Nucl Med* **55**(1), 23–29.

[17] Geng L, Wang Z, Yang X, Li D, Lian W, Xiang Z, Wang W, Bu X, Lai W, and Hu Z, et al (2015). Structure-based Design of Peptides with High Affinity and Specificity to HER2 Positive Tumors. *Theranostics* **5**(10), 1154–1165.

[18] Kameswaran M, Gota V, Ambade R, Gupta S, and Dash A (2016). Preparation and preclinical evaluation of 131 I-trastuzumab for breast cancer. *J Labelled Comp Radiopharm* **60**(1), 12–19.

[19] Engfeldt T, Orlova A, Tran T, Bruskin A, Widström C, Karlström AE, and Tolmachev V (2007). Imaging of HER2-expressing tumours using a synthetic Affibody molecule containing the 99mTc-chelating mercaptoacetyl-glycyl-glycyl-glycyl (MAG3) sequence. *Eur J Nucl Med Mol Imaging* **34**(5), 722–733.

[20] Engfeldt T, Tran T, Orlova A, Widström C, Feldwisch J, Abrahmsen L, Wennborg A, Karlström AE, and Tolmachev V (2007). 99m Tc-chelator engineering to improve tumour targeting properties of a HER2-specific Affibody molecule. *Eur J Nucl Med Mol Imaging* **34**(11), 1843–1853.

[21] Tran T, Engfeldt T, Orlova A, Sandström M, Feldwisch J, Abrahmsén L, Wennborg A, Tolmachev V, and Karlström AE (2007). 99mTc-maEEE-Z-HER2:342, an Affibody Molecule-Based Tracer for the Detection of HER2 Expression in Malignant Tumors. *Bioconjug Chem* **18**(6), 1956–1964.